JOURNAL OF COMPUTATIONAL PHYSICS 57, 137–154 (1985)

Multiple Scattering in Stratified Inhomogeneous Media

J. J. SIDOROWICH AND W. H. WELLS

Tetra Tech, Inc., 630 N. Rosemead Boulevard, Pasadena, California 91107

Received January 4, 1983; revised May 8, 1984

A method for solving the equations of radiative transfer for stratified inhomogeneous media is described. Spherical harmonics are used to simplify the Boltzmann transport equation; and a truncation scheme is implemented which essentially results in a system of equations with reduced stiffness. A response matrix formalism is developed to decouple the boundary conditions for the radiance moments from the differential equations describing the propagation properties of the medium. Several numerical examples are given. © 1985 Academic Press, Inc.

1. INTRODUCTION

Numerous methods exist for solving the problem of radiative transfer for a collimated beam of radiation incident upon a homogeneous scattering medium with one or two planar boundaries. A standard technique is to use spherical harmonics to solve the Boltzmann transport equation. This reduces the integro-differential equation into an infinite set of coupled linear differential equations of first order.

In a recent publication [1], henceforth referred to as WS, we described a novel approach for solving these coupled equations when the scattering is arbitrarily anisotropic. Anisotropic scattering means that the radiation is preferentially scattered through certain angles (usually small). However, the medium is still isotropic, which means that the individual scattering events are independent of the radiation's spatial orientation.

When the medium is inhomogeneous, conventional methods for finding solutions with exponential decay no longer apply. In this paper we describe a numerical technique that gives scattering solutions in such media with planar symmetry. Our method makes it possible to solve the differential equations describing propagation of radiation through the stratified medium without reference to the boundary conditions. The resulting system of equations can be quite stiff, and therefore difficult to solve numerically. However, our technique for making the transition from low to high degree moments permits one to use a lower order approximation, thereby reducing the stiffness of the problem. Only after the propagation characteristics of the medium have been determined do we use the boundary conditions to specify the full solution. By utilizing the formalism of WS, this technique provides good results even when the scattering is highly anisotropic.

0021-9991/85 $3.00

We demonstrate the method by solving the transient radiation field at shallow depth. This suffices to show how we manage the very large number of moments that occur in cases with small angle scattering. Further development is required to extend the method beyond several scattering lengths, where numerical instabilities are a serious problem.

As in WS, we adopt the terminology and notation appropriate for light scattering. Hence, our field quantity is radiance, which is defined as the power per steradian per unit area normal to the direction of observation. Translation of our terms into languages appropriate to other areas of study should be straightforward.

Section 2 discusses the general theory and explains how the Boltzmann equation sequence is truncated. Section 3 develops the response matrix formalism which facilitates easy solution of the differential equations. Section 4 describes various types of boundary conditions that can be used. Section 5 describes a few numerical techniques that were used in the calculation of the examples presented in Section 6.

2. General Theory [2]

A collimated beam is incident at angle ζ upon the planar boundary of a scattering medium. The medium's properties are specified by the absorption rate a and scattering function σ; a is the fractional loss of radiance per unit length along any ray and $\sigma(\psi)$ is the fraction scattered through angle ψ per unit length per unit solid angle, independent of orientation. The z-axis is normal to the boundary surface and all quantities are independent of x and y coordinates. The inhomogeneity of the scattering medium is expressed as a dependence of the scattering and absorption functions on z. We solve for radiance, $L(z, \theta, \phi)$, measured in the direction (θ, ϕ) at position z.

We expand the scattering function and radiance in terms of spherical harmonics

$$\sigma(z, \psi) = \sum_{n=0}^{\infty} \frac{2n+1}{4\pi} S_n(z) P_n(\cos\psi) \tag{1}$$

and

$$L(z, \theta, \phi) = \sum_{m=0}^{\infty} \sum_{n=m}^{\infty} (2 - \delta_{0,m}) \frac{2n+1}{4\pi} \frac{(n-m)!}{(n+m)!} L_n^m(z) P_n^m(\cos\theta) \cos m\phi \tag{2}$$

where the P_n^m are the associated Legendre functions of order m and degree n. The moments of σ and L are

$$S_n(z) = 2\pi \int_{-1}^{1} \sigma(z, \psi) P_n(\cos\psi)\, d\cos\psi \tag{3}$$

and

$$L_n^m(z) = \int_{\text{sphere}} L(z, \theta, \phi)\, P_n^m(\cos\theta)\, \cos m\phi\, d\omega \tag{4}$$

where $d\omega = d\phi\, d\cos\theta$.

In terms of these moments, the time independent monoenergetic Boltzmann equation for radiative transfer can be expressed as an infinite set of adjacently coupled differential equations for each value of m:

$$(n-m+1)\frac{\partial}{\partial z} L_{n+1}^m(z) + (n+m)\frac{\partial}{\partial z} L_{n-1}^m(z) + (2n+1) A_n(z) L_n^m(z) = 0 \tag{5}$$

where A_n is defined by

$$A_n(z) = (a + S_0) - S_n = \alpha(z) - S_n(z) \tag{6}$$

and $\alpha(z)$ is the total beam attenuation rate (absorption plus scatter).

Many techniques exist for solving the Boltzmann equation when the A_n are independent of z. A common practice is to truncate the infinite system of Eq. (5) at some value $n = N$. We then have a system of $N - m + 1$ equations that can be solved by standard analytic techniques for the low degree moments of order m.

In some formulations of radiative transfer, the spherical moments contain only the scattered radiation while the unscattered beam is a source term that feeds the scattered field. For nearly isotropic scattering this greatly reduces the number of harmonics required. However, in our case the forward scattering is so pointy that high harmonics are required in any case, and so we expand the total radiance in harmonics to avoid the use of source terms. When the results are transformed back to angular distributions the computer does not have to transform the δ-function component because it is easily recognized and subtracted out; see Appendix A.

The WS method terminates the Boltzmann equations in a way that provides expressions for high-degree moments which join naturally onto the sequence of low-degree solutions. Moments of low degree are calculated in the coordinate system with z axis perpendicular to the boundary surface, and all orders with $m \leqslant N$ are included. The moments of high-degree are calculated in a rotated coordinate system with z axis pointing in the direction of the source. In this frame of reference only the zero order (axi-symmetric) moments are needed, as discussed in WS.

To truncate the Boltzmann sequence (Eq. (5)), we solve the well-known recurrence relation

$$(n-m+1) P_{n+1}^m(\eta) + (n+m) P_{n-1}^m(\eta) = (2n+1)\eta P_n^m(\eta), \qquad \eta = \cos\zeta \tag{7}$$

for the quantity $(2n+1)$ and substitute the resulting expression into Eq. (5) to get

$$(n-m+1)(\dot{L}_{n+1}^m + R_n^m A_n L_n^m) + (n+m)(\dot{L}_{n-1}^m + Q_n^m A_n L_n^m) = 0 \tag{8}$$

where

$$R_n^m = P_{n+1}^m(\eta)/\eta P_n^m(\eta) \qquad \text{and} \qquad Q_n^m = P_{n-1}^m(\eta)/\eta P_n^m(\eta) \tag{9}$$

and we have adopted the notation $\dot{L} = \partial L/\partial z$.

We show that for n sufficiently large the two terms of Eq. (8) vanish separately:

$$\dot{L}_{n-1}^m + Q_n^m A_n L_n^m = 0 \tag{10}$$

$$\dot{L}_{n+1}^m + R_n^m A_n L_n^m = 0. \tag{11}$$

Then we use Eq. (10) with $n = N$ as the final equation of the truncated sequence. This is our P_N^m approximation in which the truncation depends on the angle of incidence through η in Eq. (9):

As $n \to \infty$, $A_n \to \alpha$, and

$$L_n^m \to \frac{P_n^m(\eta)}{\eta} \exp\left[-\int_0^z \alpha(z')\,\frac{dz'}{\eta}\right]. \tag{12}$$

This merely represents a beam of unit irradiance decaying at the rate α along the beam, dz'/η being the slant path length. Substituting this expression into Eqs. (10) and (11) shows that they are satisfied. This establishes the validity of the approximation in the large n limit, but we can do better than this. Various examples suggest that Eqs. (10) and (11) are often adequate approximations for quite moderate values of N, say 3 to 7, especially when the cause of the high harmonic content is a peak in the scattering function either in the forward or backward direction.

In the case of a forward peak, recall Eqs. (6) and (3) and the fact that $P_n(1) = 1$. For harmonics dominated by this peak, the form of Eq. (3) shows that the A_n series varies gradually so that $A_n \approx A_{n+1}$. Then we use

$$L_n = (P_n/\eta) \exp\left[-\int (A_n A_{n+1})^{1/2}\, dz'/\eta\right]. \tag{13}$$

This is a rather obvious generalization of a well-known small-angle approximation [3] for a homogeneous medium, namely $\exp(-A_n z)$, except that we claim a bit more accuracy using $(A_n A_{n+1})^{1/2}$. Substitution in Eq. (10) shows that it is satisfied to the extent that

$$A_{n-1}^{1/2} \exp\left[-\int (A_{n-1}A_n)^{1/2}\, dz/\eta\right] \approx A_n^{1/2} \exp\left[-\int (A_n A_{n+1})^{1/2}\, dz/\eta\right], \tag{14}$$

which is valid because $A_{n-1} \approx A_n \approx A_{n+1}$. A similar approximation applies to Eq. (11). (In comparing exponents, note that $A_{n-1} \approx A_{n+1}$ is usually a particularly good approximation because the Legendre polynomials P_{n-1} and P_{n+1} have the same parity.)

As another example, consider reverse scatter, in which the only scattering angle is 180°. This is the extreme case of a backscatter peak, and for the homogeneous case (A_n constant with z), it offers one of the few test cases in which an exact closed-form solution is known. This example is easily solved without spherical harmonics, but the result may be expressed in spherical moments anyhow to use as a comparison. Equations (D9) in WS gives

$$L_n = \frac{2A_{n\pm1}^{1/2}}{A_n^{1/2} + A_{n\pm1}^{1/2}} \frac{P_n}{\eta} \exp\left[-(A_n A_{n\pm1})^{1/2} \frac{z}{\eta}\right] \tag{15}$$

where $A_{n+1} = A_{n-1}$ exactly in this case. Substitution in Eqs. (10) and (11) shows that they are exactly satisfied. (For the inhomogeneous case, we would put an integral in the exponent and get an approximation with some range of validity, but this is beyond the scope of this paper.)

The two examples above indicate that Eqs. (10) and (11) are fortuitous approximations since the forward and backward scattering peaks are the ones that occur most commonly in nature. We expect that these equations would work poorly for a 90° peak (since $A_{n+1} \not\approx A_{n-1}$), but we have not investigated this because we are unaware of an application.

3. Low Degree Equations

We now return to the equations for the low degree moments. For each value of m we have Eq. (5) for $m \leqslant n < N$ and Eq. (10) for $n = N$. Since the A_n depend upon z, we must use numerical techniques to solve for the $L_n^m(z)$. However, the sets of equations are both stiff and unstable and therefore difficult to integrate. One may gain an intuitive grasp of these difficulties from the homogeneous case in which the A_n are cosntant with z. Solutions have the form

$$L_n^m = C_n^m e^{-kz} \tag{16}$$

for several eigenvalues of k. The greatest k depends on N. The lobe width of P_N^m corresponds to angular resolution of about π/N and includes rays that propagate this close to horizontal with slant paths elongated (from vertical) by the factor $\sec(\pi/2 - \pi/N) \approx N/\pi$. Such rays decay with z at rates as large as $k_{\max} = \alpha N/\pi = \alpha/(\text{ang. res.})$. At the other extreme, the least k lies between α and α and represents the smooth equilibrium distribution at great depth. So for a few degrees of angular resolution the eigenvalues, i.e., the *exponents* in the solution, may vary by a factor of 50. This wide range causes problems called stiffness. No one scale length is suitable for incrementing the solution, and a very small range of boundary conditions give usable solutions. Moreover, the negatives of k are also eigenvalues since the radiance can propagate either way ($\pm z$). This causes the set of equations to be numerically unstable because the slightest numerical imperfection is a source term that generates

many eigenvalues, including those that grow at the most rapid exponential rates and overwhelm the desired solutions.

The P_N^m approximation that we use truncates the coupled set of equations at a much smaller N, say 3 to 7, and so the *range* of exponents is an order of magnitude smaller. The equations remain stiff and unstable, but not nearly as much so. The same numerical fixes can be applied, e.g., the GEAR algorithm, or the methods of Feautrier or Rybicki [4]. However, we demonstrate that these fixes are unnecessary for problems in which the inhomogeneous layer extends only a few (3 or 4) attenuation lengths. These improvements may not be significant to workers who have ready access to a mainframe computer and a working algorithm. But for others the simplification can be significant. We used an antique microcomputer, the HP 9845A. In some instances a programmable desk calculator has sufficed.

To integrate the truncated Boltzmann equations for the L_n^m, we require a starting value at the boundary for each radiance moment. However, the radiance at the top surface is of the form

$$L(0, \theta, \phi) = L^{\text{inc}}(\theta, \phi) + L^{\text{back}}(\theta, \phi) \tag{17}$$

where L^{inc} is the radiance of the incident beam and L^{back} is the radiance that has been backscattered by the medium. Although L^{inc} is given, L^{back} is part of the solution to be determined. In fact, it depends on the conditions at the second boundary. Therefore, we need a method that bypasses these two interdependent sets of boundary values.

We define matrix functions $\Upsilon^m(z)$ that express the mth order radiance moments at depth z in terms of the values at the initial boundary surface

$$L_n^m(z) = \sum_{r=m}^{N} \Upsilon_{n,r}^m(z)\, L_r^m(z=0). \tag{18}$$

The boundary values for the elements of these $\Upsilon^m(z)$ are simply

$$\Upsilon_{n,r}^m(z=0) = \delta_{n,r}. \tag{19}$$

Substituting Eq. (18) for the $L_n^m(z)$ into the truncated Boltzmann equation sequence, Eqs. (5) and (10), gives us

$$\sum_{r=m}^{N} \left[(n-m+1) \frac{\partial}{\partial z} \Upsilon_{n+1,r}^m + (n+m) \frac{\partial}{\partial z} \Upsilon_{n-1,r}^m + (2n+1) A_n \Upsilon_{n,r}^m \right] L_r^m(0) = 0$$

$$\text{for} \quad m \leqslant n < N \tag{20a}$$

$$\sum_{r=m}^{N} \left[\frac{\partial}{\partial z} \Upsilon_{N-1,r}^m + Q_N^m A_N \Upsilon_{N,r}^m \right] L_r^m(0) = 0 \qquad \text{for} \quad n = N \tag{20b}$$

where the explicit z-dependences of the A's and Υ^m are deleted for convenience.

Since these equations must hold for aribtary incident radiance distributions, the bracketed expressions must be identically zero for each value of r. Therefore, we have found a set of differential equations which can be solved numerically to give the response matrices $\Upsilon^m(z)$ without requiring any boundary conditions on L. And so the introduction of the Υ^m matrices has simplified our task immensely by decoupling the Boltzmann equations for inhomogeneous media from the boundary conditions for the radiance moments. First, we solve the propagation problem characterized by the $\Upsilon^m(z)$; and then we impose the appropriate boundary conditions at the top and bottom surfaces.

When $N-m$ is odd, the relations extracted from Eqs. (20) can be manipulated to give expressions for the derivatives of each element of $\Upsilon^m(z)$. Letting $\dot{\Upsilon}(z) = \partial\Upsilon/\partial z$, the first ($n=m$) and last ($n=N$) equations can be written

$$\dot{\Upsilon}^m_{m+1,r} = -(2m+1)\,A_m\,\Upsilon^m_{m,r} \tag{21a}$$

$$\dot{\Upsilon}^m_{N-1,r} = -Q^m_N A_N\,\Upsilon^m_{N,r}. \tag{21b}$$

Now we use the equations for $n=m+2$ and $n=N-2$ to get

$$\dot{\Upsilon}^m_{m+3,r} = -(2(m+1)\,\dot{\Upsilon}^m_{m+1,r} + (2m+5)\,A_{m+2}\,\Upsilon^m_{m+2,r})/3 \tag{22a}$$

$$\dot{\Upsilon}^m_{N-3,r} = ((N-m+1)\,\dot{\Upsilon}^m_{N-1,r} + (2N-3)\,A_{N-2}\,\Upsilon^m_{N-2,r})/(N+m-2). \tag{22b}$$

Equations (21a) and (21b) can be inserted in the right side of Eqs. (22a) and (22b), respectively. Continuing this procedure, we see that the derivative of every element can be expressed in terms of other elements and the A_n. We start with Eqs. (21a) and (21b) and then iterate through the following equations for $j=1$ to $(N-m-1)/2$:

$$\dot{\Upsilon}^m_{m+2j+1,r} = -(2(m+j)\,\dot{\Upsilon}^m_{m+2j-1,r} + (2m+4j+1)\,A_{m+2j}\,\Upsilon^m_{m+2j,r})/(2j+1) \tag{22c}$$

$$\dot{\Upsilon}^m_{N-2j-1,r} = -((N-m-2j+1)\,\dot{\Upsilon}^m_{N-2j+1,r} + (2N-4j+1)\,A_{N-2j}\,\Upsilon^m_{N-2j,r})/(N+m-2j) \tag{22d}$$

each time replacing the derivative on the right hand side with the result of the previous iteration.

For example, in a P^0_5 calculation, the equations are

$$\dot{\Upsilon}^0_{1,r} = -A_0\,\Upsilon^0_{0,r}, \qquad \dot{\Upsilon}^0_{4,r} = -Q^0_5 A_5\,\Upsilon^0_{5,r}$$

$$\dot{\Upsilon}^0_{3,r} = -(2\,\dot{\Upsilon}^0_{1,r} + 5A_2\,\Upsilon^0_{2,r})/3 = (2A_0\,\Upsilon^0_{0,r} - 5A_2\,\Upsilon^0_{2,r})/3$$

$$\dot{\Upsilon}^0_{2,r} = -(4\,\dot{\Upsilon}^0_{4,r} + 7A_3\,\Upsilon^0_{3,r})/3 = (4Q^0_5 A_5\,\Upsilon^0_{5,r} - 7A_3\,\Upsilon^0_{3,r})/3$$

$$\dot{\Upsilon}^0_{5,r} = -(4\,\dot{\Upsilon}^0_{3,r} + 9A_4\,\Upsilon^0_{4,r})/5 = (20A_2\,\Upsilon^0_{2,r} - 8A_0\,\Upsilon^0_{0,r} - 27A_4\,\Upsilon^0_{4,r})/15$$

$$\dot{\Upsilon}^0_{0,r} = -(2\,\dot{\Upsilon}^0_{2,r} + 3A_1\,\Upsilon^0_{1,r}) = (14A_3\,\Upsilon^0_{3,r} - 8Q^0_5 A_5\,\Upsilon^0_{5,r} - 9A_1\,\Upsilon^0_{1,r})/9. \tag{23}$$

These equations can be solve by some standard iterative numerical integration routine to get values of the Υ^m at depth z.

If $N-m$ is even, Eqs. (20) comprise a singular system of equatons which cannot be inverted for the $\dot{Y}$. Hence, the method fails in this case.

4. Boundary Conditions

Once the $\Upsilon^m(z)$ are known, the only task remaining is to determine the values of the low degree radiance moments at the boundary surface. We now describe a set of boundary conditions appropriate for a slab of finite thickness. We also discuss conditions for an infinite slab, or half space. It is not our intention to provide an exhaustive study of boundary conditions in general; we are only concerned with demonstrating the utility of the Υ^m formalism in a few specific examples.

4.1. *Finite Slab*

We consider a slab of thickness Z_0 surrounded by vacuum. The boundary conditions that we use are the Marshak conditions [5] appropriately oriented for each of the vacuum-scatterer interfaces. These conditions follow from the assertion that, since the vacuum does not produce any backscatter, the scattered radiance at each surface is zero in the out-looking direction. For example, looking up from the top surface $L^{\text{back}}=0$ and Eq. (17) gives

$$L(z=0, \theta<90^\circ, \phi)=L^{\text{inc}}(\theta, \phi). \tag{24}$$

If we express both of these functions as spherical harmonic expansions, their difference is equal to

$$\sum_{m'=0} \sum_{n=m'} \frac{(2-\delta_{0,m'})}{4\pi}(2n+1)\frac{(n-m')!}{(n+m')!}(L_n^{m'}(0)-L_n^{\text{inc},m'}) \times P_n^{m'}(\mu)\cos m'\phi=0 \tag{25}$$

where $\mu=\cos\theta$.

Multiplying this equation by $P_r^m(\mu)\cos m\phi$ and integrating over the up-looking hemisphere, we get

$$\int_0^{2\pi} d\phi \int_0^1 d\mu \sum_{m'=0} \sum_{n=m'} \frac{(2-\delta_{0,m'})}{4\pi}(2n+1)\frac{(n-m')!}{(n+m')!} \times (L_n^{m'}(0)-L^{\text{inc},m'}_n)\, P_n^{m'}(\mu)\, P_r^m(\mu)\cos m'\phi\cos m\phi = \sum_{n=m}(n+\tfrac{1}{2})\frac{(n-m)!}{(n+m)!}(L_n^m(0)-L^{\text{inc},m}_n)\, K^m_{n,r}=0 \tag{26}$$

where [6]

$$K^m_{n,r}=\int_0^1 P_n^m(\mu)\, P_r^m(\mu)\, d\mu=\frac{P_n^{m+1}(0)\,P_r^m(0)-P_n^m(0)\,P_r^{m+1}(0)}{(n-r)(n+r+1)}. \tag{27}$$

$K^m_{n,r}$ is easily computed by using the relation

$$P^m_n(0) = \mathrm{Re}[(-1)^{(n-m)/2}] \frac{(n+m-1)!!}{(n-m)!!}. \tag{28}$$

Equation (26) is used for various values of r, between m and N, inclusive, each value providing one equation for the unknown surface radiance moments. However, since the P^m_n constitute a doubly complete basis when integrated over a hemisphere, we can only get one-half of the $N-m+1$ linearly independent relations needed to fully determine all the $L^m_n(0)$.

The other half of the equations can be derived from Marshak conditions at the lower boundary. There is no radiation from the vacuum incident on this face of the scatterer. Therefore, we have

$$L(z = Z_0, \theta > 90°, \phi) = 0. \tag{29}$$

Once again we express L in terms of spherical harmonics and multiply by $P^m_r(\mu) \cos m\phi$. However, we now integrate over the down-looking hemisphere to get

$$\sum_{n=m} (n+\tfrac{1}{2}) \frac{(n-m)!}{(n+m)!} (-1)^{n+r} K^m_{r,n} L^m_n(Z_0) = 0. \tag{30}$$

The factor $(-1)^{n+r}$ follows from the fact that

$$P^m_n(\mu) = (-1)^{m+n} P^m_n(-\mu). \tag{31}$$

We now substitute Eq. (18) for $L^m_n(Z_0)$ in Eq. (30). The result is

$$\sum_{j=m} \sum_{n=m} (n+\tfrac{1}{2}) \frac{(n-m)!}{(n+m)!} (-1)^{n+r} K^m_{r,n} \Upsilon^m_{n,j}(Z_0) L^m_j(0) = 0. \tag{32}$$

This equation constitutes the other half of the conditions that, in conjunction with Eq. (26), determine the surface values of the radiance moments.

The summations over n in Eqs. (26) and (30) should run to infinity. However, the impracticality of such a calculation requires termination of the summations at some finite number of terms. The simplest solution uses just the low-degree moment terms and stops at $n = N$. Additional terms for the effects of high-degree moments can be included if N is particularly small or if higher precision is desired.

We must also decide which values of r are to be used in Eqs. (26) and (32). We follow the usual procedures of using those values of r such that $m + r$ is odd. (These harmonics vanish at $\theta = 90°$; thus, they ignore the rather meaningless rays that skim the surface in favor of those that penetrate.)

4.2. *Half-Space*

When the slab's thickness is infinite, the Marshak conditions can still be applied at the boundary of the half-space, and the resulting equations will be the same as Eq.

(26). However, the lack of a lower boundary necessitates our finding conditions to be imposed on the asymptotic forms of the radiance moments. Assuming that the medium gradually becomes homogeneous, i.e., $A_n(z \to \infty) = \text{constant}$, we expect that in the large z limit the solutions will take the form of the decay eigensolutions appropriate for a homogeneous medium specified by the limiting values of the A_n.

In order to develop this idea further, we briefly review the formalism of these eigensolutions as developed in WS. For a homogeneous medium, we showed that the radiance moments can be expressed in the form

$$L_n^m(z) = \sum_j B(k_j)\, C_n^m(k_j) \exp(-k_j z) \tag{33}$$

where the $C_n^m(k_j)$ are eigenvector solutions of Eqs. (5) and (10) associated with the decay eigenvalues k_j. In a P_N^m approximation, the $C(k_j)$ are $(N-m+1)$-dimensional vectors and there are $(N-m+1)/2$ values of k^2. The summation over j is a summation over the distinct eigensolutions, with the contribution of each eigensolution being specified by the $B(k_j)$. Each $C(k_j)$ has a conjugate vector $\bar{C}(k_j)$ such that

$$\sum_{n=m}^{N} \bar{C}_n^m(k_i)\, A_n\, C_n^m(k_j) = H\delta_{i,j} \tag{34}$$

where H is a normalization constant. The weighting factors, $B(k_i)$, can then be found by multiplying Eq. (33) by $\bar{C}_n^m(k_i) A_n H^{-1}$ and summing over n:

$$B(k_i)\, e^{-k_i z} = H^{-1} \sum_{n=m}^{N} \bar{C}_n^m(k_i)\, A_n L_n^m(z). \tag{35}$$

The decay eigenvalues come in $\pm$ pairs. In WS, we showed that for each eigenvector $C_n^m(k_j)$ decaying exponentially as $e^{-k_j z}$ there also exists an exponentially increasing eigensolution $C_n^m(-k_j)\, e^{+k_j z}$ where $C_n^m(-k_j) = (-1)^n\, C_n^m(k_j)$. However, these solutions must be deleted since the radiance must go to zero at $z = \infty$.

If we now return to the inhomogeneous half-space, it is clear that in the homogeneous limit we must have no contribution from the eigensolutions of the asymptotic region that grow exponentially. In other words, the weighting factors for these physically inadmissable solutions must be zero, i.e.,

$$\lim_{z\to\infty} B(-k_i)\, e^{+k_i z} = H^{-1} \sum_{n=m}^{N} \bar{C}_n^m(-k_i)\, A_n L_n^m(z \to \infty) = 0. \tag{36}$$

Substituting $(-1)^n\, \bar{C}_n^m(k_i)$ for $\bar{C}_n^m(-k_i)$ and Eq. (18) for L_n^m, Eq. (36) becomes

$$\sum_{r=m}^{N} \sum_{n=m}^{N} (-1)^n\, \bar{C}_n^m(k_i)\, A_n\, \Upsilon_{n,r}^m(z \to \infty)\, L_r^m(0) = 0. \tag{37}$$

This equation is used for each of the $(N-m+1)/2$ positive k_i. Therefore, Eq. (37)

provides one-half of the equations necessary to determine the surface radiance moments. As was mentioned before, the other half of the equations come from Eq. (26).

Now, although Eq. (37) looks adequate for our needs, we must recall that the $\Upsilon^m(z)$ can only be solved numerically, and hence the quantities $\Upsilon^m_{n,r}(z \to \infty)$ are not obtainable in practice. However, if the half-space becomes homogeneous at some finite depth, i.e., if $A(z \geqslant Z_0) = \text{constant}$ for some finite Z_0, then Eq. (37) can be used by putting $z \to \infty \equiv Z_0$.

In this way, we can analyze the problem of a homogeneous half-space covered by an inhomogeneous slab of finite thickness. We solve the response matrix for the inhomogeneous region and then use Eq. (37) at the slab-half-space interface. Since the medium is homogeneous beyond this interface, the radiance moments begin to decay exponentially as the WS propagation eigenvectors of the half-space and take the asymptotic forms expected. In fact, the deep field solution can be expressed in the form of Eq. (33) by using Eq. (35) at the interface.

5. Computational Techniques

Once the radiance moments have been determined, we must reconstruct the radiance according to Eq. (2). However, this involves two infinite summations which make the calculations non-trivial. In this section, we outline several techniques that greatly simplify the computations.

As was mentioned in Section 2, the high-degree moments are calculated in a rotated coordinate system with z-axis aligned in the direction of the source. In this reference frame, only the zero-order moments are needed and so Eq. (2) becomes

$$4\pi L(z, \theta, \phi) = \sum_{m=0}^{N} \sum_{n=m}^{N} (2 - \delta_{0,m})(2n + 1) \frac{(n-m)!}{(n+m)!} L_n^m(z)\, P_n^m(\cos\theta) \cos m\phi + \sum_{n=N+1}^{\infty} (2n + 1)\, L_n'(z)\, P_n(\cos\zeta \cos\theta + \sin\zeta \sin\theta \cos\phi) \qquad (38)$$

where the prime denotes that the high-degree harmonics are calculated in the rotated frame, and the argument of P in the second sum is the cosine of the polar angle from the source axis.

We still have an infinite sum over n remaining. In WS, we terminated this sum by convolving the radiance with a narrow blur function. This function must be very narrow for angles near a sharp peak but may be broad for diffuse backscatter. The convolution is effected by multiplying the radiance moments by the corresponding moments of the blur function.

We have also developed another method that has better convergence properties. First, each term in the sum is expanded in powers of $S_n z$. Then all terms of a given order in $S_n z$ are grouped together. Finally, analytic expressions are found for the

transforms of these groupings. The analysis can be continued to any order desired, depending upon the convergence rate required and the perseverance and cleverness of the researcher. This method is elaborated in Appendix A.

Because we use delta-function sources, the solutions we find contain delta-function components corresponding to unscattered radiation, namely $L^{\text{inc}} \exp(-\alpha z/\eta)$. It is poor practice to leave this in the numerical transform, since its high harmonics merely generate numerical errors. Therefore, we subtract it out of Eq. (38) before transforming.

6. Numerical Examples

We present three examples that apply the techniques described in the previous sections. The first is a contrived test case for which the exact solution is known, and provides a verification of the method. We then present two examples with a realistic scattering function. In one case, we work with a finite slab; and then we look at the problem of a homogeneous half-space covered by such a slab.

It should be pointed out that we have not greatly concerned ourselves with the intricacies of performing the required numerical integrations to great depth. All of the examples presented in this section were calculated using a simple fourth order Runge–Kutta algorithm, with no specific modifications for dealing with stiffness. For problems where the integrations' stability is an important factor, modifications of the basic matrix equations may be required to get useful solutions.

6.1. *Test Case*

We begin this example by arbitrarily specifying what the radiance distribution is throughout the slab. Equation (5) can then be used to give expressions for the $A_n(z)$. We must work this example with the radiation at normal incidence ($\eta = 1$) so that $L_n^m = 0$ for $m \neq 0$. Otherwise we would have a different set of $A_n(z)$ for each value of m.

At the top surface, we take the radiance to be

$$L(0, \theta, \phi) = \delta(\mu - \eta)\, \delta(\phi) + H(-\mu) \tag{39}$$

where $\mu = \cos\theta$, $\eta = \cos\zeta$ and $H(\mu)$ is the step function

$$H(\mu) = \begin{matrix} 1, & \mu > 0 \\ 0, & \mu < 0. \end{matrix}$$

At the bottom surface, we take the radiance to be

$$L(Z_0, \theta, \phi) = (1 - \sin\theta)\, H(\mu). \tag{40}$$

These surface distributions are plotted in Fig. 1 (solid line).

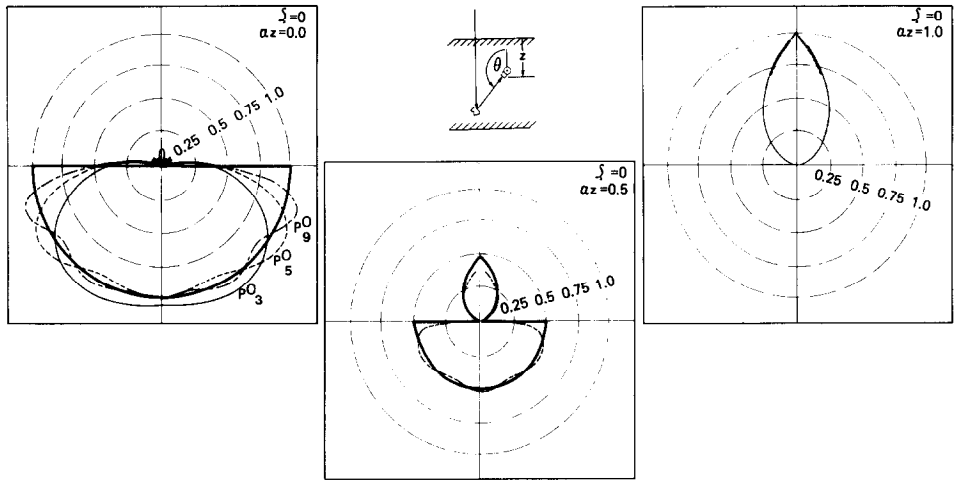

FIG. 1. Radiance distributions for slab of section 6.1. $\alpha z = 0$, 0.5, 1.0. P_5^0 approximation.

The choice of these distributions is arbitrary: we simply selected functions that are somewhat plausible and can easily be expanded in spherical harmonics, as demonstrated in Appendix B.

For simplicity, we let $L_n(z)$ vary linearly between the two limits in Eqs. (39) and (40):

$$L_n(z) = L_n(0) + zD_n. \tag{41}$$

In other words, $\partial L_n/\partial z = D_n$ is a constant, given by

$$D_n = [L_n(Z_0) - L_n(0)]/Z_0. \tag{42}$$

Substituting Eq. (41) for the L_n into Eq. (5), we get the Boltzmann equation in the form

$$(n+1)D_{n+1} + nD_{n-1} + (2n+1)A_n(z)[L_n(0) + zD_n] = 0. \tag{43}$$

We can now solve for the $A_n(z)$:

$$A_n(z) = -\left(\frac{(n+1)D_{n+1} + nD_{n-1}}{(2n+1)[L_n(0) + zD_n]}\right). \tag{44}$$

The scattering function $\sigma(\psi)$ given by Eq. (1) for these A_n is probably unphysical with negative values for some ψ; but we do not care since our only purpose is to provide a mathematical demonstration of the accuracy of the approximations used.

Figure 1 displays the radiance distribution calculated from a P_5^0 approximation

using Eqs. (23). The three polar plots give radiance for the top surface, the midplane, and the bottom, respectively. At the top, results of P_3^0 and P_9^0 approximations are also included for comparison.

6.2. *Finite Slab*

We now work the problem of a slab of unit thickness with scattering function given by

$$\sigma(z, \psi) = \left(\frac{3 - 2z}{4\pi}\right) [2(1 - \cos \psi)]^{-1/2}, \qquad 0 \leqslant z \leqslant 1, \tag{45}$$

and $a = 1$. This function has a strong peak for scattering in the forward direction ($\psi = 0$); in fact, it is an integrable singularity. This generates many high harmonics that demonstrate the utility of the method.

Another reason for using this function is the simple form of its moments. Using Eqs. (3) and (6), we find that

$$S_n(z) = \frac{3 - 2z}{2n + 1} \qquad \text{and} \qquad A_n(z) = \frac{8n + 1 - 4nz}{2n + 1}. \tag{46}$$

We use an incident radiance distribution of the form

$$L^{\text{inc}} = \delta(\phi)\, \delta(\mu - \eta)/\eta \Rightarrow L^{\text{inc},m}_n = P_n^m(\eta)/\eta. \tag{47}$$

At normal incidence this becomes

$$L^{\text{inc},m}_n = P_n^m(1) = \delta_{0,m}.$$

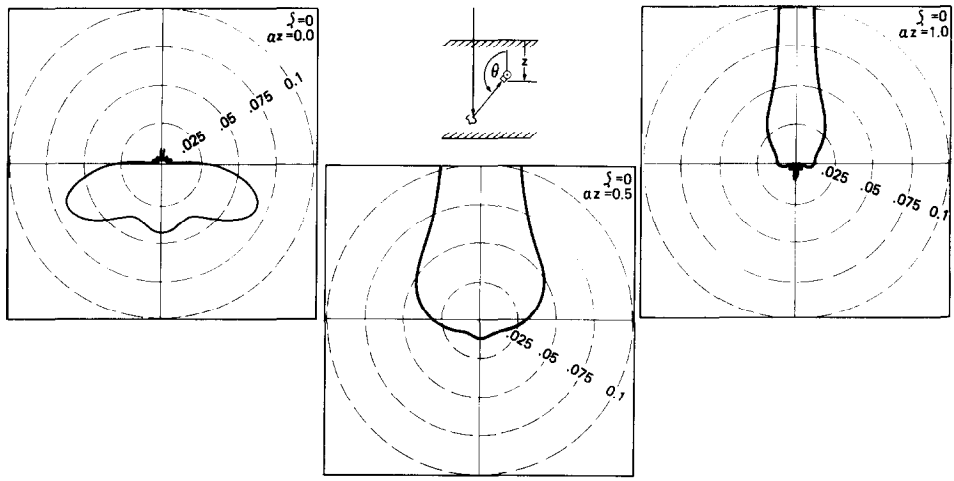

FIG. 2. Radiance distributions for normal incidence ($\zeta = 0$) on slab of unit thickness with σ given by Eq. (45). $\alpha z = 0$, 0.5, 1.0. P_3^0 approximation.

We then use these normal incidence moments in the Marshak conditions of Eqs. (26) and (32).

The results of a P_5^0 approximation are plotted in Fig. 2. The radiance distributions are shown at both boundaries and midway through the slab. At the bottom surface there is a noticeable amount of noise in the outlooking direction. This can be attributed to having neglected the terms for high-degree moments in the boundary conditions at this surface. These noise lobes could be reduced by using a higher N approximation or by using high-degree terms in Eqs. (32).

6.3. *Half-Space*

We now look at a half-space with the scattering function given by Eq. (45) for $z \leqslant 1$, and for $z > 1$ $\sigma(z, \psi) = (4\pi)^{-1} [2(1 - \cos \psi)]^{-1/2} = \sigma(1, \psi)$. In both regions, $a = 1$.

This is equivalent to the problem of a homogeneous half-space covered by the slab of the last example.

Following the arguments of Section 4.2, we can calculate the asymptotic decay eigenvectors by using the techniques of WS with the $A_n(z = 1) = A_n(\infty)$. The boundary conditions of Eq. (37) can then be used, along with the top-surface Marshak conditions of Eq. (26), to determine the radiance moments.

We computed the radiance resulting from a collimated beam (Eq. (47)) incident on the half-space at $\zeta = \arccos \eta = 40°$. Figure 3 shows polar plots in the plane of incidence at the top of the slab, the midpoint, and the bottom. A simple but useful check of the results follows from the principle of reciprocity. According to this principle, the value of the radiance should remain unchanged under an interchange of the source and detector. Several points are included in Fig. 3 which indicate that the computed results are consistent with reciprocity.

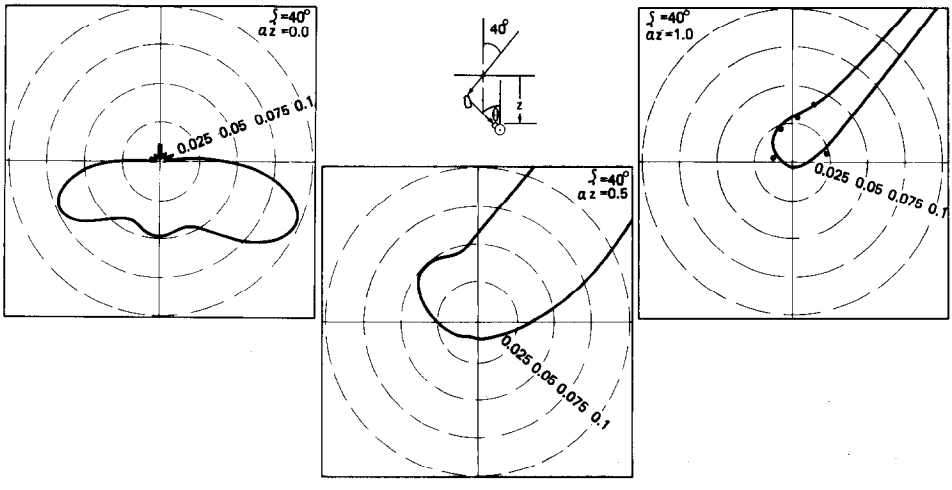

FIG. 3. Radiance distributions in the plane of incidence for $\zeta = 40°$. Medium is the half-space described in Section 6.3. $\alpha z = 0$, 0.5, 1.0, Approximations: P_5^0, P_4^1, P_5^2, P_4^3, P_5^4.

Appendix A

Consider the infinite sum

$$f(\mu) = \sum_{n=0}^{\infty} \frac{2n+1}{4\pi} P_n(\mu)\, e^{-A_n z}. \tag{A1}$$

Apart from a few terms of low degree, this is the same sum that must be evaluated numerically [see Eq. (38)]. Using Eq. (6) we have

$$f(\mu) = e^{-\alpha z} \sum_{n=0}^{\infty} \frac{2n+1}{4\pi} P_n(\mu) \left[1 + S_n z + \frac{(S_n z)^2}{2!} + \frac{(S_n z)^3}{3!} + \cdots\right]. \tag{A2}$$

If each term in the square bracket is summed over n separately, the convergence is more rapid for the higher powers of $(S_n z)$. The first two terms, which converge especially slowly, are recognized as

$$\sum_{n=0}^{\infty} \frac{2n+1}{4\pi} P_n(\mu)[1 + S_n z] = \delta(1-\mu) + z\sigma(\theta). \tag{A3}$$

So we subtract off this part and compute Eq. (A1) in the form

$$f(\mu) = e^{-\alpha z}[\delta(1-\mu) + z\sigma(\theta)] + \sum_{n=0}^{\infty} \frac{2n+1}{4\pi} P_n(\mu)[e^{-A_n z} - e^{-\alpha z}(1 + S_n z)]. \tag{A4}$$

We have continued this sort of analysis up to the $(S_n z)^2$ and $(S_n z)^3$ terms in Eq. (A2), when considering the scattering function of Eq. (45). We inserted the moments given in Eq. (46) into Eq. (A2); and found functions with transforms that displayed the same dependence on n as the quadratic and cubic terms in the sum. Of course, this continuation to higher orders in the expansion parameter depends upon the form of the specific scattering function being considered and can get very complicated. We are presently compiling a table of transforms that may be useful for this sort of work, and we hope to include it as part of a future publication.

Appendix B

In this appendix, we calculate the moments of the boundary radiances given in Eqs. (39) and (40).

It proves helpful to first consider the integral

$$I_n^m = \int_0^1 P_n^m(\mu)\, d\mu. \tag{B1}$$

We begin with the recurrence relation

$$(n-m+1)\,P_{n+1}^m(\mu)+(n+m)\,P_{n-1}^m(\mu)=(2n+1)\,\mu P_n^m(\mu) \tag{B2}$$

and the derivative formula

$$(1-\mu^2)\,\frac{d}{d\mu}\,P_n^m(\mu)=(n+1)\,\mu P_n^m(\mu)-(n-m+1)\,P_{n+1}^m(\mu). \tag{B3}$$

Integrating these from 0 to 1 and using Eq. (B1) gives

$$(n-m+1)\,I_{n+1}^m+(n+m)\,I_{n-1}^m=(2n+1)\int_0^1 \mu P_n^m(\mu)\,d\mu \tag{B4}$$

and

$$\int_0^1 (1-\mu^2)\left(\frac{d}{d\mu}\,P_n^m(\mu)\right)d\mu=(n+1)\int_0^1 \mu P_n^m(\mu)\,d\mu-(n-m+1)\,I_{n+1}^m. \tag{B5}$$

Integrating by parts on the left side of this last equation gives us

$$\int_0^1 \mu P_n^m(\mu)\,d\mu=[(n-m+1)\,I_{n+1}^m-P_n^m(0)]/(n-1). \tag{B6}$$

Substituting this expression into Eq. (B4), we get

$$I_{n+1}^m=\frac{(2n+1)\,P_n^m(0)+(n-1)(n+m)\,I_{n-1}^m}{(n+2)(n-m+1)}. \tag{B7}$$

This recursion formula, along with Eq. (28), can be used to find the various I_n^m that are needed.

Now we return to the boundary expressions. First, we solve for the moments at the top surface. From Eqs. (39) and (B1)

$$\begin{aligned}\frac{L_n(0)}{2\pi}&=\int_0^1 \delta(\mu-\eta)\,P_n(\mu)\,d\mu+\int_{-1}^0 P_n(\mu)\,d\mu\\&=P_n(\eta)+(-1)^n\int_0^1 P_n(\mu)\,d\mu\\&=P_n(1)+(-1)^n\,I_n^0\end{aligned}$$

where, from Eq. (B7),

$$I_n^0=\begin{cases}\delta_{0,n} & \text{for } n \text{ even}\\ \dfrac{(-)^{(n-1)/2}\,(n-2)!!}{(n+1)!!} & \text{for } n \text{ odd.}\end{cases}$$

For the lower boundary, we use Eq. (40) to find

$$\frac{L_n(z)}{2\pi} = \int_0^1 P_n(\mu)\, d\mu - \int_0^1 (1-\mu^2)^{1/2}\, P_n(\mu)\, d\mu.$$

Using the recurrence relation

$$P^1_{n+1}(\mu) - P^1_{n-1}(\mu) = (2n+1)(1-\mu^2)^{1/2}\, P_n(\mu)$$

we see that

$$\begin{aligned}\frac{L_n(z)}{2\pi} &= I^0_n - \frac{1}{2n+1}\,(I^1_{n+1} - I^1_{n-1}) \\ &= I^0_n - (P^1_n(0) - I^1_{n-1})/(n^2+2n).\end{aligned}$$

ACKNOWLEDGMENT

We are grateful to the U.S. Office of Naval Research, Code 425C, for financial support.

REFERENCES

1. W. H. WELLS AND J. J. SIDOROWICH, *Ann. Phys. (N.Y.)* **144** (1982).
2. Several standard texts that can be referred to are: A. M. WEINBERG AND E. P. WIGNER, "The Physical Theory of Neutron Chain Reactors," Univ. of Chicago Press, Chicago, 1958; K. J. CASE AND P. F. ZWEIFEL, "Linear Transport Theory," Addison–Wesley, Reading, Mass., 1967; B. DAVISON AND J. B. SYKES, "Neutron Transport Theory," Oxford Univ. Press (Clarendon), London/New York, 1957.
3. M. C. WANG AND E. GUTH, *Phys. Rev.* **84** (1951), 1092–1111.
4. A convenient description can be found in: D. MIHALAS, "Stellar Atmospheres," Freeman, San Francisco, 1978.
5. R. E. MARSHAK, *Phys. Rev.* **71** (1947), 443.
6. N. G. SHABDE, *Bull. Calcutta Math. Soc.* **29** (1937), 33–40.